ARL-TR-9077 ● SEP 2020

Simulation of Optical Coupling between Tapered Fibers and Nanoscale Whispering Gallery Mode Microresonators

by Priscilla Lopez and Dashiell LP Vitullo

NOTICES

Disclaimers

The findings in this report are not to be construed as an official Department of the Army position unless so designated by other authorized documents.

Citation of manufacturer's or trade names does not constitute an official endorsement or approval of the use thereof.

Destroy this report when it is no longer needed. Do not return it to the originator.

ARL-TR-9077 ● SEP 2020

Simulation of Optical Coupling between Tapered Fibers and Nanoscale Whispering Gallery Mode Microresonators

Priscilla Lopez
University of Texas at San Antonio

Dashiell LP Vitullo
Computational and Information Sciences Directorate, CCDC Army Research Laboratory

REPORT DOCUMENTATION PAGE

Form Approved
OMB No. 0704-0188

1. REPORT DATE *(DD-MM-YYYY)*	2. REPORT TYPE	3. DATES COVERED (From - To)
September 2020	Technical Report	06/01/2020–08/07/2020

4. TITLE AND SUBTITLE
Simulation of Optical Coupling between Tapered Fibers and Nanoscale Whispering Gallery Mode Microresonators

5a. CONTRACT NUMBER

5b. GRANT NUMBER

5c. PROGRAM ELEMENT NUMBER

6. AUTHOR(S)
Priscilla Lopez and Dashiell LP Vitullo

5d. PROJECT NUMBER

5e. TASK NUMBER

5f. WORK UNIT NUMBER

7. PERFORMING ORGANIZATION NAME(S) AND ADDRESS(ES)
CCDC Army Research Laboratory
ATTN: FCDD-RLC-NT
Adelphi, MD 20783-1138

8. PERFORMING ORGANIZATION REPORT NUMBER
ARL-TR-9077

9. SPONSORING/MONITORING AGENCY NAME(S) AND ADDRESS(ES)

10. SPONSOR/MONITOR'S ACRONYM(S)

11. SPONSOR/MONITOR'S REPORT NUMBER(S)

12. DISTRIBUTION/AVAILABILITY STATEMENT
Approved for public release; distribution is unlimited.

13. SUPPLEMENTARY NOTES
ORCID IDs: Priscilla Lopez, 0000-0003-2307-8751; Dashiell LP Vitullo, 0000-0001-8797-9968

14. ABSTRACT
We investigate use of Lumerical finite-difference, time-domain (FDTD) software for numerical simulation of optical coupling between a tapered optical fiber and a surface nanoscale axial photonic microresonator device with nanoscale radius variation. Simulations utilizing reasonable computational resources (per simulation: approximately 15-h runtime, approximately 10 GB of random access memory) produce spectrograms with good modal structure and demonstrate the feasibility of this approach.

15. SUBJECT TERMS
SNAP microresonators, surface nanoscale axial photonics, tapered optical fiber, optical coupling, simulation, finite-difference time-domain, FDTD, nanoscale

16. SECURITY CLASSIFICATION OF:			17. LIMITATION OF ABSTRACT	18. NUMBER OF PAGES	19a. NAME OF RESPONSIBLE PERSON
a. REPORT	b. ABSTRACT	c. THIS PAGE			Dashiell LP Vitullo
Unclassified	Unclassified	Unclassified	UU	18	19b. TELEPHONE NUMBER (Include area code) (301) 394-0403

Contents

List of Figures

List of Tables

Acknowledgments

This research was sponsored by the US Department of Defense's Historically Black Colleges and Universities and Minority-Serving Institutions Summer Program.

1. Introduction

Optical microresonator technology is a promising platform for controlling light in optical networks with a wide variety of applications including controlling the travel time of light with optical delay lines,[1] directing light into specific channels with optical switching,[2] storing light with optical buffering,[3–4] generating precise optical references as sources for optical frequency combs,[5–6] and interfacing with atomic quantum systems.[7] Microresonators can be interfaced to optical fiber networks with high ideality[8] and low loss[9] through the use of tapered optical fibers. This is a particularly promising capability for quantum networking applications, where the no-cloning theorem prevents amplification,[10] making loss a substantial challenge. Surface nanoscale axial photonics (SNAP) technology, which we focus upon here, boasts ultrahigh intrinsic quality factors ($Q \sim 10^8$), subangstrom fabrication precision,[11] and slow tunability.[12] Detailed modeling capability is an important tool for realization and extension of these applications.

Control of resonant mode structure beyond a single axial series can be informed by a detailed 3-D resonator model, which is the use-case for which Lumerical's finite-difference, time-domain (FDTD) software is designed. SNAP microresonators are typically modeled using a 1-D potential that is limited to modeling one axial series at a time. These resonators have a typical extent of approximately 100 μm along a fiber, but only nanoscale height variation over that range.[13–14] The necessity of small mesh sizes to properly account for the nanoscale variation over a relatively large surface indicates that care must be taken to make an accurate simulation that can be run with a practical amount of memory in a reasonable amount of time.

Herein, we investigate both the feasibility of simulating SNAP devices with nanoscale radius variation using 3-D Lumerical models and the computational resource requirements necessary for this task. We model a simple waveguide and nanoscale resonator system with 25-nm bump height. We calculate the transmission spectra through the waveguide in multiple simulations, where the waveguide is positioned at a different transverse location along the resonator in each simulation, to calculate a spectrogram. We find the expected modal structure and preliminary indication that detailed SNAP simulations with FDTD software are feasible. This will serve as the foundation for further work into FDTD's ability to model linear and nonlinear SNAP device operation, the effects of variation of 3-D taper and resonator geometry therein, and the fast temporal dynamics of light in these systems.[15]

2. 3-D Modeling with FDTD

Lumerical's FDTD software uses a finite-difference, time-domain analytical method to model optical systems by solving time-dependent Maxwell's equations.[16] This is accomplished using a discretized mesh with one time dimension and three spatial dimensions. The six electromagnetic components of Maxwell's equations are separated into transverse electric (TE) and transverse magnetic (TM) equations, which are then solved at different locations on a spatial and temporal grid.[17–19] Utilizing this method in the Device Suite Lumerical software package, we are able to model the optical properties of a tapered fiber waveguide and microbottle resonator coupled system.

The simulation is situated in a rectangular volume with dimensions $69 \times 53 \times 22$ microns. Any space not occupied by an object is filled with air using a model that includes temperature effects on its material's parameters. The temperature is set to 300 K and the refractive index of the surrounding medium is set to 1. The maximum simulation duration limit is set to 45,000 fs. The simulation will complete before this duration limit is reached if the fraction of energy left in the simulation region falls below the autoshutoff threshold. The minimum value for this threshold was set to 10^{-6} when setting the FDTD volume to ensure the simulation would only complete when a majority of the energy was gone from the simulation volume. A boundary of virtual layers known as perfectly matched layers were set to surround and close the simulation region. These boundaries also act as an absorbing layer surrounding the region stopping and unwanted reflections from causing interference.

To test the capabilities of FDTD in modeling SNAP devices, a tapered fiber with a waist radius of 0.5 micron and a total length of 85 microns is modeled by grouping a cylinder with a truncated cone on each side as one structure. The cone has a 10-micron radius at its thickest point. A microbottle resonator is created with a length of 25 microns and a maximum resonator bump size of 25 nm by combining a cylinder and an elliptical toroid (Fig. 1). Microresonator mode localization is set by the effective radius variation of a fiber, which depends on variation of both the physical radius and refractive index,[13] but we vary the physical radius only here and use a uniform refractive index model for silica (SiO_2) from E Palik's measurements of optical constants of solids.[20] The region with nanoscale radius variation is highlighted in red in Fig. 1 to make it visible. These objects are placed next to each other with the tapered fiber touching the resonator along the "bump" of the resonator.

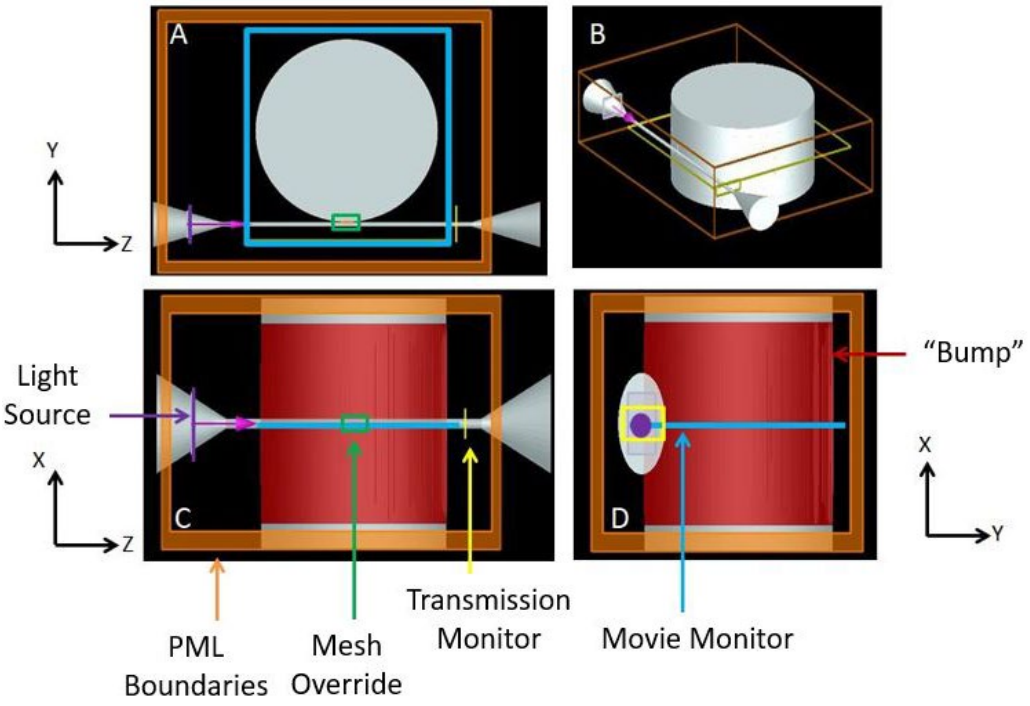

Fig. 1 Visualization of the setup indicating the positions of the components by color such as the light source, monitors, boundaries, mesh override, and "bump" or curved area due to the slight radius change, as highlighted in red; a) top profile view, b) perspective view, and c) and d) side profile views

The light source in the system is modeled by a simulation object called the SourceMode, which is used to compute and inject a guided mode of a structure into the region. While the object has the capabilities to compute multiple modes for this situation, the fundamental guided TE mode is computed for the tapered fiber and input light is launched into this mode. The pulse type of the source is set to broadband and a bandwidth of 0.17 THz is used, which sets the wavelength range to 1553.8–1555.1 nm. Before these values were chosen, a test run over a large wavelength range was completed to determine the area of interest. The light source pulse length is set to 3000 fs so interference between incident and circulated light can be observed.

The default grid spacing in the 3-D spatial mesh is set based on the specified wavelength range for the simulation and the "mesh accuracy" setting. Mesh resolution fine enough to capture details of the nanoscale variation must be balanced against computational resource requirements (memory and runtime). The mesh accuracy option gives a range of settings from 1 to 8 with higher settings corresponding to more spatial mesh points per wavelength. A mesh accuracy of 1 will set the simulation to create a total of 6 mesh points per wavelength in the spatial

grid while a mesh accuracy of 5 corresponds to 22 mesh points per wavelength. A mesh accuracy of 1 is chosen to set the default grid spacing, but we use FDTD's mesh override feature to create a refined mesh in the coupling region. The rectangular region spans $1.5 \times 0.2 \times 0.2$ microns (see Fig. 1) containing mesh points with separations of 10 nm in each direction. Monitor objects are placed to designate what properties of light should be calculated and recorded, and where this should take place. A movie monitor is placed through the middle of the system, as shown in blue in Fig. 1. This specific monitor is set to capture the path of light during the simulation, allowing us to verify the coupling between the fiber and resonator. At the end of the tapered fiber (highlighted in yellow in Fig. 1), a frequency-domain field and power monitor is placed in order to obtain the transmission spectrum by recording data at 1000 frequency points within the wavelength range set by the light source.

FDTD estimates the memory requirements of a simulation from the configuration before execution (Table 1). The memory requirements here, if not explicitly stated as a file size, are for the amount of random access memory (RAM) needed. The simulations with the model in the smaller wavelength range $\Delta\lambda_s$ that spans 1553–1555 nm require a total of 7.179 GB of RAM, divided among the following categories: initialization and mesh, 3.779 GB; running the simulation, 2.267 GB; data collection, 755 MB; and monitor data saved to fsp file, 378 MB. If we change the mesh accuracy to a higher setting, for example, to a mesh accuracy of 2, the total memory requirement jumps to 19.75 GB. Changing the mesh override size has a smaller impact, for example, changing the physical mesh spacing from 10 to 5 nm increases the total memory requirement to only 11.617 GB. Parameters such as the simulation time and the number of frequency points in the transmission spectrum do not change the memory requirements as dramatically. Doubling the number of frequency points only raises the memory requirement by 1.5 GB. Increasing the maximum simulation duration by 5000 fs (to 50,000 fs) demonstrates a similar increase. Each simulation using the smaller wavelength range ($\Delta\lambda_s$) requires 12–16 h of runtime to complete and generate 371-MB output data files. The longer wavelength range ($\Delta\lambda_l$) simulation required runtimes in the range of 14–18 h with a total memory requirement of 11.816 GB and an output data file size of 1.44 GB.

Table 1 Simulation memory requirements (RAM)

Usage	$\Delta\lambda_s$	$\Delta\lambda_l$
Initialization and mesh	3.779 GB	3.848 GB
Running simulation	2.267 GB	3.435 GB
Data collection	755 MB	3.022 GB
Monitor data	378 MB	1.511 GB
Total	7.179 GB	11.816 GB

A common approach in the experimental investigation of SNAP microresonators is to measure a "spectrogram".[14] These are typically made experimentally by placing the taper in contact with the resonator at one x-position, and then moving the taper to another x-position and repeating the transmission measurement, and repeating this process to map out coupling between the resonator and the taper.[21] This method is duplicated by running the simulations with the taper positioned at multiple x-locations to simulate a spectrogram. Simulations were run over two wavelength ranges: $\Delta\lambda_s$ as previously described and a second larger wavelength range $\Delta\lambda_l$ spanning 1548.4–1560.5 nm with a bandwidth of 1.5 THz. To increase the frequency grid for the larger wavelength range, we run an additional simulation where the number of frequency points collected in the transmission monitor is raised from 1000 to 4000.

Experimentally, the taper can be placed against the resonator and will not pass through it. A challenge in the simulation is that there is no restriction preventing objects from overlapping and the coupling is very sensitive to the positioning, so the positioning between the objects needs to be precisely controlled. The taper is centered over the middle of the resonator bump when positioned at $x = 0$, and it makes contact with the resonator in this position when $y = -20.524$ μm. We simulate transmission there and at additional positions every 2 μm along the x-axis. The y value for contact is calculated using

$$\frac{x^2}{a} + \frac{(y + 19.999)^2}{b} = c, \tag{1}$$

where $a = 10$ μm^2, $b = 0.025$ μm^2, and $c = 1$. After finding these points, the fiber is set and graphically inspected in the user interface to verify there are no gaps and adjusting the position up to the tenth of a nanometer, if necessary. For each simulation, the fiber is set to a new location 2 microns away from the previous and once again graphically verified to have no gaps between the objects.

3. Results

The movie monitor produces a video of light traveling through the waveguide exhibiting expected behavior, including coupling into the resonator and circulating, followed by interference between circulated light and transmitting light in the coupling region. We simulate the transmission spectrum of the modeled system over two wavelength ranges (Fig. 2). In the first set of data, the measurements are taken with the tapered fiber positioned at the center or the peak of the radius variation of the resonator (indicated in Fig. 2a as $x = 0$), and at a grid of x positions spaced 2 microns apart.

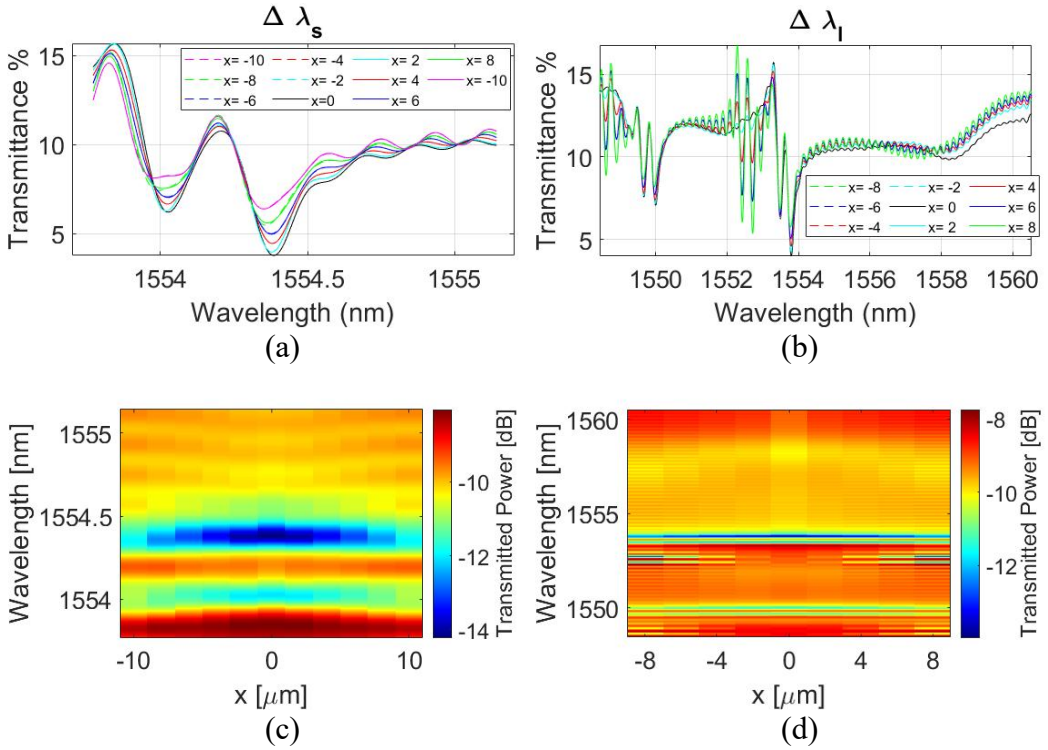

Fig. 2 a) Transmission spectra over a small bandwidth range $\Delta\lambda_s$ when the tapered fiber is located at the labeled position, where x indicates the distance in microns along the x-axis (Fig. 1) of the taper center from the center of the resonator bump. b) Transmission spectra for the larger wavelength range simulation $\Delta\lambda_l$. c) Spectrogram of the smaller wavelength range $\Delta\lambda_s$. d) Spectrogram of the larger wavelength range spectra $\Delta\lambda_l$.

From these spectra, we observe the expected behavior that the transmission dip is deepest and widest at $x = 0$, and the dips get shallower and narrower as $|x|$ increases.[13] We also observe that the corresponding points on either side of the center have the same spectra with less than 0.1% difference between the amplitudes of the transmission, verifying the symmetry of the configuration. This has great importance for future work, as with verified symmetry, we can utilize symmetric boundaries in the simulation. By adding a symmetric boundary, the simulation

region will be cut in half reducing memory and simulation time. A similar spectra is shown in the second set of data, where the dip at the central point is the deepest and widest, seen in Fig. 2b, except we see in the spectra measured at $x = 2$ and higher, there is now a development of additional dips, suggesting coupling to additional resonator modes not seen in the smaller wavelength range. Data are exported to MATLAB for spectrogram generation. In Fig. 2c, we see a distinct axial mode in the data from the smaller wavelength data correlating to the dips in the transmission spectra. The data set of the larger wavelength range is also displayed as a spectrogram (Fig. 2d) and we see additional resonance dips from coupling to additional resonator modes.

4. Conclusion

Using Lumerical's FDTD software we are able to successfully model a simple version of a SNAP device, obtain transmission spectra, and make spectrograms exhibiting reasonable modal structure. Through this modeling, we gained insight into the fundamental requirements of using this software on microsized systems with nanoscale surface variation. This research lays the foundation for more efficient models that utilize the symmetry verified herein to simulate experimental systems and paves the way toward investigation of relationships among distinct series of axial modes, the effects of deformations in 3-D geometry, and nonlinear device operation.

5. References

1. Sumetsky M. Delay of light in an optical bottle resonator with nanoscale radius variation: dispersionless, broadband, and low loss. Phys Rev Lett. 2013;111:1.
2. O'Shea D, Junge C, Pöllinger M, Vogler A, Rauschenbeutel A. All-optical switching and strong coupling using tunable whispering-gallery-mode microresonators. Appl Phys B. 2011;105:129.
3. Burmeister EF, Blumenthal DJ, Bowers JE. A comparison of optical buffering technologies. Opt Switch Netw. 2008;5:10.
4. Yoshiki W, Honda Y, Tetsumoto T, Furusawa K, Sekine N, Tanabe T. All-optical tunable buffering with coupled ultra-high Q whispering gallery mode microcavities. Sci Rep. 2017;7:10688.
5. Kippenberg TJ, Holzwarth R, Diddams SA. Microresonator-based optical frequency combs. Science. 2011;332:555.
6. Dvoyrin V, Sumetsky M. Bottle microresonator broadband and low-repetition-rate frequency comb generator. Opt Lett. 2016;41:5547.
7. O'Shea D, Junge C, Volz J, Rauschenbeutel A. Fiber-optical switch controlled by a single atom. Phys Rev Lett. 2013;111:193601.
8. Spillane SM, Kippenberg TJ, Painter OJ, Vahala KJ. Ideality in a fiber-taper-coupled microresonator system for application to cavity quantum electrodynamics. Phys Rev Lett. 2003;91:043902.
9. Rokhsari H, Vahala KJ. Ultralow loss, high Q, four port resonant couplers for quantum optics and photonics. Phys Rev Lett. 2004;92:253905.
10. Wootters W, Zurek W. A single quantum cannot be cloned. Nature. 1982;299:802–803.
11. Toropov NA, Sumetsky M. Permanent matching of coupled optical bottle resonators with better than 0.16 GHz precision. Opt Lett. 2016;41:2278–2281.
12. Vitullo DLP, Zaki S, Gardosi G, Mangan BJ, Windeler RS, Brodsky M, Sumetsky M. Tunable SNAP microresonators via internal ohmic heating. Opt Lett. 2018;43:4316–4319.
13. Sumetsky M. Theory of SNAP devices: basic equations and comparison with the experiment. Opt Express. 2012;20:22537.
14. Sumetsky M. Nanophotonics of optical fibers. Nanophotonics. 2013;2:393.

15. Jiang X, Shao L, Zhang SX, Yi X, Wiersig J, Wang L, Gong Q, Lončar M, Yang L, Xiao YF. Chaos-assisted broadband momentum transformation in optical microresonators. Science. 2017;358:344.

16. FDTD product reference manual. Vancouver (Canada): Lumerical Inc.; 2020 [accessed 2020]. https://support.lumerical.com/hc/en-us/articles/360033154434-FDTD-product-reference-manual.

17. Gedney S. Introduction to the finite-difference time-domain (FDTD) method for electromagnetics. In: Introduction to the finite-difference time-domain (FDTD) method for electromagnetics. San Rafael (CA): Morgan & Claypool; 2011.

18. Product overview. Vancouver (Canada): Lumerical Inc.; 2020 [accessed 2020]. https://www.lumerical.com/products/.

19. Sullivan DM. Electromagnetic simulation using the FDTD method. New York (NY): IEEE Press Series; 2000.

20. Palik ED. Handbook of optical constants of solids: III. San Diego (CA): Academic Press; 1998.

21. Vitullo DLP, Zaki S, Jones DE, Sumetsky M, Brodsky M. Coupling between waveguides and microresonators: the local approach. Opt Express. 2020;28:25908.

List of Symbols, Abbreviations, and Acronyms

1-D	one-dimensional
3-D	three-dimensional
FDTD	finite difference, time domain
RAM	random access memory
SiO_2	silica
SNAP	surface nanoscale axial photonics
TE	transverse electric
TM	transverse magnetic

1 (PDF)	DEFENSE TECHNICAL INFORMATION CTR DTIC OCA
1 (PDF)	CCDC ARL FCDD RLD DCI TECH LIB
1 (PDF)	CCDC ARL FCDD RLC NT D VITULLO